Mon. Not. R. Astron. Soc. **279**, 165–170 (1996)

On the wings of broad Hα emission in active galactic nuclei

P. Romano,[1] T. Zwitter,[1] M. Calvani[2] and J. Sulentic[3]

[1] *University of Ljubljana, Department of Physics, Jadranska 19, 61000 Ljubljana, Slovenia*

[2] *Osservatorio Astronomico di Padova, Vicolo dell'Osservatorio 5, I-35122, Padova, Italy*

[3] *University of Alabama, Department of Physics and Astronomy, Tuscaloosa, AL 35487, USA*

Email: promano@astrpd.pd.astro.it, tomaz.zwitter@uni-lj.si, calvani@astrpd.pd.astro.it, giacomo@merlot.astr.ua.edu

Accepted 1995 September 29. Received 1995 September 29; in original form 1995 July 25

ABSTRACT

The wings of broad emission lines in active galactic nuclei (AGN) arise from matter moving at extreme velocities. We use a large sample (≈ 100 spectra) of Hα emission line profiles to study the curvature and asymmetry properties of the broad-line wings. Our sample is strongly weighted towards radio-loud objects (4 to 1). Our study includes a comparison of the red- and blue-wing fits for each object. We compare the results with the predictions of various models for the broad-line region (BLR).

Profile velocity displacements are common in our sample with almost equal numbers of red- and blueshifts observed at zero intensity. We find that approximately half the objects show different (i.e. log-like or power-law) fits to the red and blue wings. This population strongly favours power-law fits on the blue and log fits on the red side. This may be evidence for multiple BLR emission components with fundamentally different velocity distributions in these objects. Among the objects where both wings are fitted by the same function we find equal numbers with matching log and power-law fits. The power-law fitted profiles tend to be narrower and more blueshifted than the log fitted ones in the matched fitted samples.

Key words: line: formation – line: profiles – galaxies: active – galaxies: nuclei – quasars: emission lines – galaxies: Seyfert.

1 INTRODUCTION

Two kinds of extreme velocities are observed in the broad emission lines of AGN: (1) velocity displacement of all or part of the line profile (up to ± 4000 km s^{-1}) and (2) velocity broadening of the line profile (up to FWHM ∼ 23 000 km s^{-1}). The first is an ensemble velocity measured relative to the local rest frame and is assumed to be a pure kinematic feature. The latter is the velocity distribution of individual radiating clouds, which is superposed on the former, and is more of a statistical mechanical property. Each component provides clues about and constraints for models of the BLR emitting region. The simplest, and hence most attractive, single-force models for the BLR emitting region involve pure rotational or radial motions. Most frequently discussed models include: (a) a spherically symmetric ensemble of radially moving clouds, (b) a bipolar flow of radially moving clouds and (c) a geometrically thin accretion disc. The principal physical parameters of such models include the volume emissivity ϵ, the radial dependence of the bulk velocity $v(r)$ and the inner ($r_{\rm in}$) and outer ($r_{\rm out}$) radii of the emitting region.

Accretion disc models make rather definite predictions about the shape of the emission lines. In simple models they are expected to be double-peaked over the most likely range of viewing angles (e.g. Dumont & Collin-Souffrin 1990). Relativistic accretion discs (Chen, Halpern & Filippenko 1989) can also account for moderate line asymmetries which are frequently observed. In double-peaked profiles the blue peak is expected to be stronger due to relativistic beaming and the entire profile is affected by the gravitational redshift (i.e. the velocity of the centroid at zero intensity should be positive). The biconical scenario is able to explain an even wider range of observed asymmetries by adjusting the optical thickness and geometrical obscuration of the emitting clouds (Zheng, Binette & Sulentic 1990; Marziani, Calvani & Sulentic 1992). The difficulties with attempting to fit any of the above models to a majority of the data have strengthened the idea of a composite BLR. Our study supplements the observational evidence for composite BLR emission lines.

Attempts to compare the global BLR profile shape with various model predictions are hampered by the small numbers of high-quality observations. Additional complications involve the necessity to subtract narrow-line components and Fe II contamination. This has led to a statistical approach in most modern studies. Numerous authors (Gaskell 1982; Espey et al. 1989; Corbin 1990) investigated the general properties of line asymmetries and shifts and compared them with models. Refined approaches have included: (1) studies of the profile at different depths in the lines (de Robertis 1985; Sulentic 1989; Boroson & Green 1992) and (2) interpercentile velocity measurements (Stirpe 1991).

In this study we concentrate on the wings of the broad emission lines. Our study quantifies both extreme velocity components mentioned above through measures of the profile centroid and width at zero intensity. The wings of the line originate from matter moving with extreme velocity with respect to the local rest frame (or with respect to the kinematic centre of the emitting region in cases where the line shows a global velocity displacement). Thus, in general, the emission arises from a spatially limited region so that the results are insensitive to the unknown radial dependence of the emissivity. This is especially true for rotationally dominant models such as accretion discs where the wings arise close to the inner edge of the emitting region. The constraint appears to be even stronger for radial models because of recent evidence that line wings respond to continuum changes at the same time as the rest of the profile (e.g. Clavel et al. 1991). A particular innovation in this study involves an attempt to compare the red and blue wings in each profile. That comparison is motivated by the growing evidence that BLR features may be composite.

In the next section we present our profile analysis rationale and procedures. In Section 3 we describe the comparison between theory and observation with special emphasis on accretion disc models. We also present a general discussion of wing shapes and the efficacy of simple functions for fitting them. Conclusions are presented in Section 4.

2 DATA PROCESSING AND ANALYSIS

We studied two Hα samples: (1) Stirpe (1990, hereafter S90) and (2) Eracleous & Halpern (1994, hereafter EH94). The former sample consists of 29 Seyfert 1 and low-redshift QSOs, optically selected from the Véron-Cetty & Véron (1984) catalogue where they are classified as Broad Emission Line AGNs. A few 'classical' objects (van Groningen 1984) were included in S90 in order to search for possible variations in profile shape. The S90 sample has a magnitude limit of $m_V \leqslant 16.5$ and a redshift limit of $z \leqslant 0.35$, and extends over a range of 9 orders of magnitude in absolute luminosity (from $M_V = -16$ to $M_V = -25$ assuming $H_0 = 75$ km s^{-1} Mpc^{-1} and $q_0 = 0$). All but five objects in S90 are radio-quiet.

The EH94 sample is a large (n=74) collection of broad-line radio galaxies and radio-loud quasars selected from the Véron-Cetty & Véron (1989) catalogue. It includes the majority of such objects with $z \leqslant 0.4$. The 3C and PKS sources included are all powerful FR II radio galaxies (Faranoff & Riley 1974). Arp 102B and 1E 0450.3-1817 are also included although they belong to the FR I class (three orders of magnitude weaker than FR II). However they are still unusually radio-bright compared with other Seyfert galaxies.

Neither sample claims to be complete; the former is biased towards nearby Seyferts and the latter clearly consists of radio-loud objects that often show complex or even double-peaked line profiles. Some of these have been fitted with simple relativistic accretion disc models (i.e. disc-like emitters, EH94).

Our focus on the profile wings has the practical advantage over global studies that it does not depend on the determination of any particular fractional height in the line under consideration. This allows us to increase the sample of quasars available for study by considering numerous spectra available in the literature that do not allow an accurate determination of the peak of the BLR component. This statement is really only true if Hα is the line under study. The wings of Hβ (as well as C IV: Marziani et al. 1996) are more uncertain because of Fe II contamination. A study of Hα is also attractive because it is the highest signal-to-noise ratio (S/N) broad line observable in the optical and because the narrow components only moderately contaminate the profile of the broad component: the narrow Hα and both [N II] components are confined to the region within ± 3000 km s^{-1} from the line centre; the [O I] $\lambda\lambda 6300, 6364$ and the [S II] $\lambda\lambda 6716, 6731$ lines are very narrow compared with their distances from the centre of the Hα profile, as well.

Table 1. Redshifts that differ from EH94. See text.

Source Name	z	Source Name	z
1E 0450.3-1817	0.0615	PKS 0235+023	0.2073
3C 93	0.3584	PKS 0312-77	0.2257
3C 390.3	0.0546	PKS 0340-37	0.2854
3C 206	0.1977	PKS 0846+10	0.3656
B2 0742+31	0.4613	PKS 1302-103	0.279
B2 1028+31	0.178	PKS 1725+045	0.2968
B2 1719+35	0.283	PKS 1914-45	0.364
PKS 0214+10	0.4070	PKS 2227-399	0.318

Two parameters can be extracted from the models and compared with observations in a straightforward manner: (i) the wing curvature and, in the case of convex wings, (ii) the velocity at zero intensity. Terminal velocities from the red and blue wings can also be combined to calculate the full width and line shift at zero intensity. We describe the shape of the observed Hα wings by fitting them with a variety of simple functions (log, linear, square root and a range of power laws). Reliable terminal velocities could not always be measured for wings that were well fitted by a power law.

The analysis of profile wings followed the following steps.

(i) The centre of the broad Hα profile was determined from the centroids of narrow Hα and the [O I] lines. Detailed studies of narrow-line redshifts (Vrtilek, Carleton & Huchra 1981; Wilson & Heckman 1985) show that these lines usually agree within 100 km s^{-1} with other estimates of the systemic redshift. Table 1 lists our derived redshifts for objects that did not agree with EH94 (their tables 2 and 3) at the 10^{-3} level.

(ii) Only the blue and red parts of the continuum-subtracted profile outside ± 3000 km s^{-1} were measured in this study.

(iii) Narrow-line contributions were removed and the red and blue parts of the profile below 60 per cent of the maximum intensity were considered to be the wing components. This is the only point in our calculations where we used an intensity-dependent selection criterion. We also experimented with other intensity limits (e.g. 40 per cent) and found that the results were virtually unchanged.

(iv) The curvatures of the red and blue wings were fitted with various analytical functions. Ten different functions were used:

$$I(v) = \begin{cases} I_0 \sqrt{1 - v/v_0} \\ I_0 (1 - v/v_0) \\ I_0 \log(v/v_0) \\ I_0 \, v^{-\alpha} & \alpha = 1...7. \end{cases} \quad (1)$$

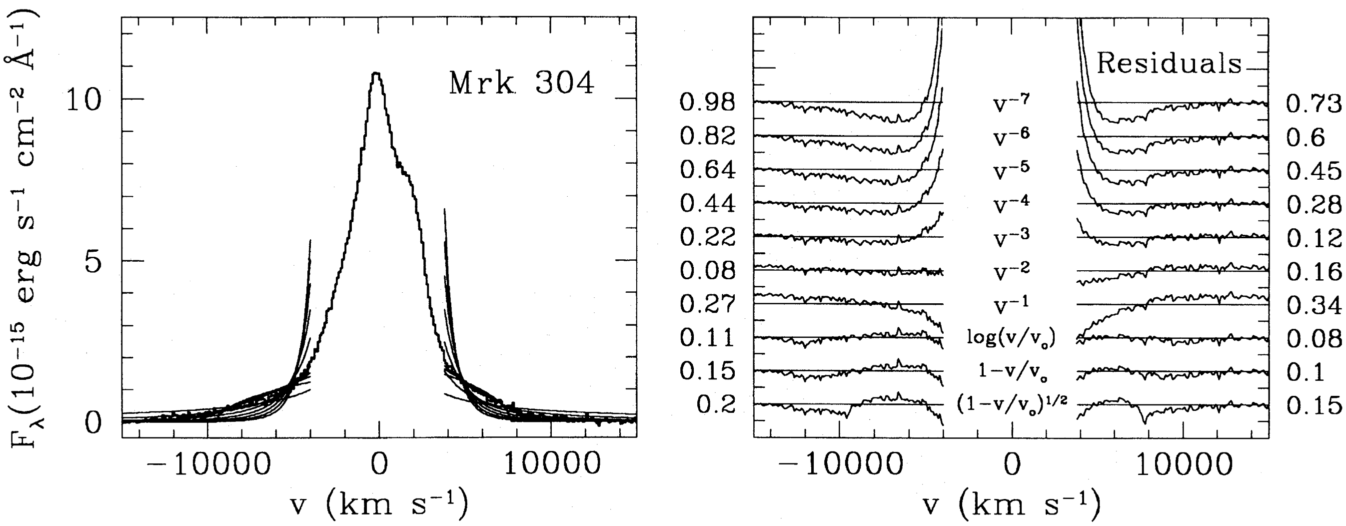

Figure 1. Analytical fits to the wings of a typical Hα profile from our sample (Mrk 304). The observed profile with superimposed fits is shown on the left. The residuals for different fits are shown on the right. Scales are the same but the residuals are vertically offset for clarity. The numbers along the right-hand graph indicate standard deviations (in arbitrary units).

Here $I(v)$ is the line intensity with respect to the line centre at velocity v. The above functions can be arranged in two groups: log-like (the first three) and power-law. Log-like wings have a well-defined terminal velocity v_0 while power laws do not. Reliable values for parameters that are dependent on terminal velocity could therefore not be determined for some objects with strong power-law curvature. The functions (1) cover the range of convex and concave shapes that might be expected for the wings of emission lines. The results of a sample fit are shown in Fig. 1.

(v) Profiles with full width at zero intensity FWZI $\leqslant 12\,000$ km s^{-1} were excluded because of the narrowness of the remaining wings. Additional objects were excluded from the sample because of a low S/N or difficulties in obtaining a unique fit to the wings. After these alterations the final sample included 65 objects.

3 RESULTS

The results of our profile wing analysis can be directly compared with the shapes predicted by various models. We focus here on comparisons with radiating accretion disc models because of the considerable theoretical and observational effort that has been reported in the last few years. The shape of the wings appears to be considerably more robust than the peak in disc models. The EH94 sample was constructed in a search for objects with Balmer line emission that could be well fitted by disc models. We consider first the domain of shifts and profile widths at zero intensity followed by considerations on wing shapes.

Fig. 2 shows the velocity of the centroid at zero intensity Δv versus the full width at zero intensity FWZI for the objects from the S90 and EH94 samples. The FWZI has been calculated as the sum of the terminal velocity of the red and the blue wings and the centroid as half their difference. Predictions for a relativistic accretion disc model (Chen et al. 1989) are plotted. Solid lines mark the relation between the centroid velocity at zero intensity Δv and FWZI for fixed values of the disc inclination i. The horizontal dotted lines give the values of the expected centroid velocity at ZI for a given value of the disc's inner radius $r_{\rm in}$ (in units of GM/c^2). The relations

$$\mathrm{FWZI} = 2\,\frac{c\,\sin i}{\sqrt{r_{\rm in} - 3}} \tag{2}$$

and

$$\Delta v = c\left(\frac{1}{\sqrt{1 - 3/r_{\rm in}}} - 1\right) \tag{3}$$

follow directly from equation (13) of Chen et al. (1989).

The disc model predictions do not appear to match well the observed properties of the profile wings. This is a stronger constraint than the presence or absence of double peaks but the uncertainties of measurements at zero intensity are also larger. They are not, however, large enough to move many more disc-like emitters into the model domain. Two points deserve special mention.

(1) Even among disc-like emitters (filled circles in Fig. 2) there are objects with moderate but definite blueshifts of the centroid at zero intensity. This is in contrast to a general theoretical prediction for a gravitational redshift that should be particularly prominent in the wings of the line. Five out of twelve disc-like emitters show a centroid at half maximum that is redshifted with respect to the one at zero intensity (cf. table 6 in EH94).

(2) The remaining disc-like emitters generally favour high inclination angles if equations (2) and (3) are used to interpret the properties of their wings. This does not agree with EH94 who obtained low inclination angles when fitting the shape of the entire BLR profile of disc-like emitters.

Of course it was already clear from the residuals of disc models fits (plotted in fig. 4 of EH94) that the relativistic accretion disc models could not explain the extent and asymmetry of the observed wings. The line broadening introduced by EH94 does not seem to change these conclusions because it cannot appreciably shift the centroid at zero intensity.

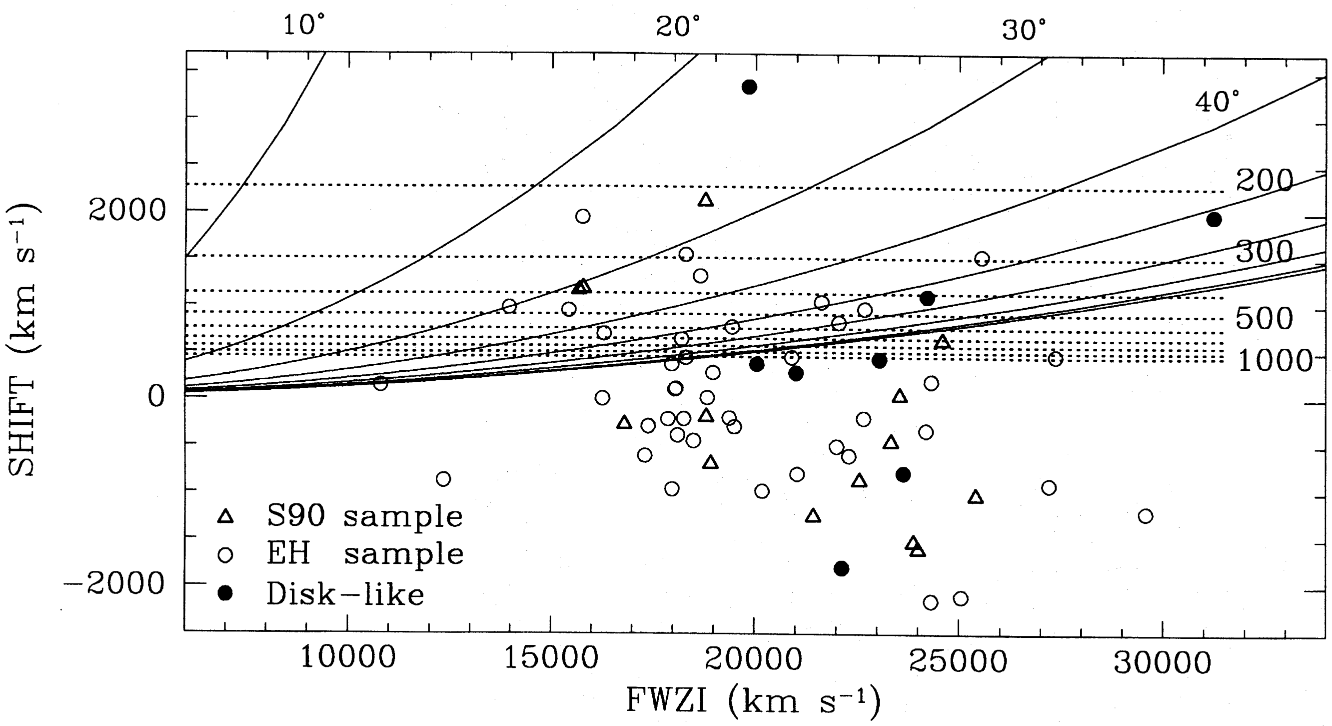

Figure 2. Comparison of accretion disc model predictions and observational data. The solid lines mark *loci* for a relativistic accretion disc (Chen et al. 1989) at inclinations between 10° and 90°. The horizontal dotted lines give the values of the expected velocity of the centroid at zero intensity for a given disc inner radius (in units of GM/c^2). The observations are S90 (triangles) and EH94 (circles). The filled circles represent the disc-like emitters, i.e. double-peaked profiles that EH94 fitted with disc models.

There are two reasons for distinguishing between fits to the red and blue wings of profiles: (1) they are often different and (2) there is increasing evidence for multiple components in high-S/N spectra of both high- and low-ionization broad lines. We find equal numbers of objects (n=17) where both wings are fitted by either a log-like or a power-law profile. A large number (n=21) show a power-law blue wing and a log-like red one. The opposite situation (blue log + red power-law) is rare (n=5). Fig. 3 shows the distributions of the four fit classes in the domain of FWZI versus centroid zero intensity. Four points are worth mentioning.

(i) Disc-like emitters show no preference for any profile wing class.

(ii) Radio-quiet objects (indicated by boxes) show a preference for different fits to the red and blue wings (always blue power-law and red log-like). Most of the objects from S90 were-radio quiet but such objects are strongly under-represented in this study. In our small sample radio-quiet objects do not appear to be appreciably narrower at ZI than the 'broad-line' radio galaxies.

(iii) The centroid of the pure power-law fitted sample shows a displacement towards smaller FWZI and blueshift at zero intensity. The mean full width and centroid values (all in km s^{-1}) at zero intensity are FWZI=2.20×10^4, Δv=+85 and FWZI=1.99×10^4, Δv=−194 for pure log-like and power-law samples respectively.

(iv) There is evidence for a correlation between shift and width in the pure power-law sample in the sense that larger FWZI corresponds to larger blueshift.

It is clear from visual inspection of many high-S/N line profiles for both C IV and Hβ (see Marziani et al. 1996) that the broad-line emission contains multiple components with different kinematic, and therefore probably geometrical, properties. This is evident in profiles that show well-defined inflections. The clearest cases often suggest a blueshifted component in C IV and a redshifted one in Hβ coupled to a stronger and less shifted central feature. Many profiles do not show such a structure. Our wing analysis should be particularly sensitive to the presence of a secondary weaker component (see e.g. Corbin 1995 and references therein). We interpret the mixed fit samples as the most likely candidates for composite BLR profiles.

The lack of unambiguous signals in the wing analysis is not surprising. The comparison is useful because it represents a reasonably large sample analysed in a systematic way. However it became clear early in this study that simple functional fits were often unable to describe the observed profiles adequately. Some profiles with visually different wings were still formally best fitted by the same kind of function. Of course, visual impressions are guided by the entire line profile while the analysis considered only the wings. Fig. 4 presents the distribution of mean residuals for the different functions fitted to the red and blue sides. Fig. 4 shows that the smallest residuals correspond to profiles that could be fitted by either a logarithmic or a power-law function with α=2. Often the difference between the residuals of these two fits was not significant although Fig. 4 shows that log fits are better on average. There are other smaller populations where either a log-like or a power-law fit was clearly preferred, but the

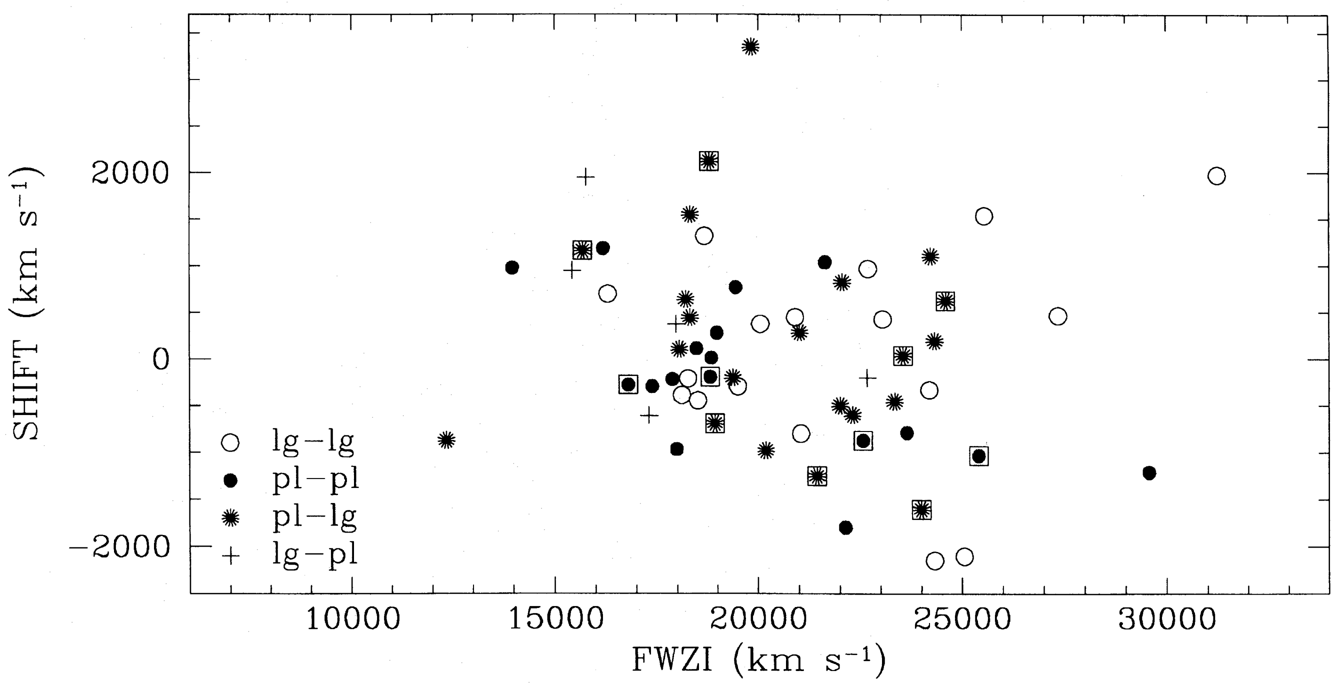

Figure 3. The distribution of FWZI versus line shift at zero intensity for different profile wing classes. Symbols are identified in the lower left corner (e.g. lg-pl means that the blue wing was fitted by a log-like function while the red one was fitted by a power law). Symbols for radio-quiet objects are enclosed in boxes. A few symbols are slightly offset to avoid overlap. Fewer objects are shown here than in Fig. 2 because reliable wing fits were not possible in all cases.

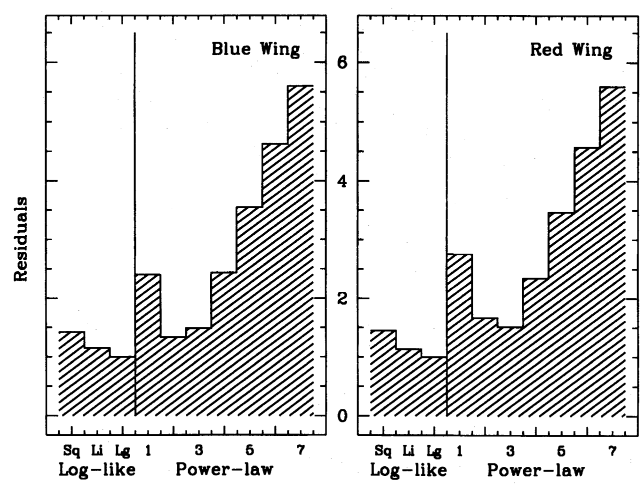

Figure 4. The distribution of mean residuals for the fits to the blue and red wings of the line profiles for all analytical fits attempted. Sq, Li and Lg indicate square root, linear and logarithmic respectively. The order of the power-law fits is also labelled. Residuals are normalized to the best-fitting value.

majority are ambiguous. This suggests two approaches for future work: (1) more complex functions are needed to fit the wings, and (2) complex profiles can be deconvolved and the separate components fitted. Both approaches are becoming possible as more high-quality spectra are obtained.

4 CONCLUSIONS

We made simple analytical fits to the wings in the broad-line component of Hα for $\sim$ 100 AGNs. We also studied the behaviour of the full width and centroid velocity at zero intensity. Approximately equal numbers of red- and blue-shifted zero intensity centroids were found (12 redshifts and 7 blueshifts are observed with shifts exceeding 10^3 km s^{-1}). The zero intensity shift does not correlate with FWZI except possibly for objects with pure power-law wing fits. The distribution in the shift versus FWZI domain for disc-like emitters and other radio-loud objects does not follow the predictions of simple accretion disc models.

The situation is more ambiguous for the wing fits. Naively one expects square-root wings from an emitting Keplerian disc and logarithmic profiles for emission from radially moving clouds (Penston et al. 1990). This is an oversimplification because the radial dependences of emissivity and velocity have an important effect on the wing shape. This can be seen in fig. 4 of Robinson (1995) where power-law wings are favoured when the emissivity ϵ varies as r^{-2} (accretion discs) and r^{-3} (radial inflow or outflow). Log-like wings are produced for a Keplerian disc when $\epsilon \propto r^{-3}$ and for radial models when $\epsilon \propto r^{(-3+2p)}$ where p is defined by the radial dependence of velocity $v(r) \propto r^p$.

There is a weak correlation between FWZI and the analytical function that gives the best fit. Narrow profiles tend to have (α=2–3) power-law wings. Wide profiles are better represented by logarithmic wings yielding a well-defined terminal (asymptotic) velocity. This agrees with the results of Penston et al. (1990) who favoured power-law wings. The objects that they studied are quite narrow compared with our sample which is populated with broad-line radio galaxies. This would place them at the lower end of our FWZI sample distribution and would favour power-law fits.

What determines whether an object shows power-law or log-like wings? The central source luminosity could be the critical parameter. Lower luminosity sources should show weak power-law wings that can be produced either by a centrally illuminated accretion disc or by an outflow that ceases to emit Hα before it reaches terminal velocity. Radial inflow is an equivalent possibility. In cases where the central source is stronger, the existence of a terminal velocity and the fact that an accretion disc generally does not fit the observed properties favour models involving a strong and bright outflow. In this case the bulk of the emission comes from matter at the terminal velocity. Variation of optical thickness and partial obscuration of the far-side jet by the central structure (e.g. an accretion disc, Zwitter & Calvani 1994) can naturally explain both kinds of observed asymmetries in these wide BLR profiles.

We find many objects with different fits to the red and blue wings. This corresponds to the impression gained from visual inspection of line profiles and from the large number with significant asymmetries. The evidence strongly favours a multiple-component BLR in a significant number of AGNs. This evidence is by no means restricted to radio-loud objects.

We conclude that in many cases the simple analytic functions are inadequate to describe the profile wings. More complex analytical fits to the profile wings and profile deconvolution studies are needed to advance our understanding of BLR structure.

ACKNOWLEDGMENTS

We are grateful to G. Stirpe and to M. Eracleous for providing access to their data in digital form. We also thank M. Eracleous and P. Marziani for many useful comments and discussions. PR thanks the staff of the Department of Physics, University of Ljubljana, for their kind hospitality and acknowledges the financial support from the Government of the Republic of Slovenia through a post-graduate scholarship. MC and TZ acknowledge the financial support of the European Economic Community for Cooperation in Science and Technology with Central and Eastern European Countries (contract no. ERBCIPDCT940028).

REFERENCES

Boroson T. A., Green R. W., 1992, ApJS, 80, 109
Chen K., Halpern J. P., Filippenko A. V., 1989, ApJ, 339, 742
Clavel J. et al., 1991, ApJ, 366, 64
Corbin M. R., 1990, ApJ, 357, 346
Corbin M. R., 1995, ApJ, 447, 496
de Robertis M., 1985, ApJ, 289, 67
Dumont A. M., Collin-Souffrin S., 1990, A&A, 229, 313
Eracleous M., Halpern J. P., 1994, ApJS, 90, 1 (EH94)
Espey B. R., Carswell R. F., Bailey J. A., Smith M. G., Ward M. J., 1989, ApJ, 342, 666
Faranoff B. L., Riley J. M., 1974, MNRAS, 167, 31P
Gaskell C. M., 1982, ApJ, 263, 79
Marziani P., Calvani M., Sulentic J. W., 1992, ApJ, 393, 658
Marziani P., Sulentic J. W., Dultzin-Hacyan D., Calvani M., Moles M., 1996, ApJS, in press
Penston M. V., Croft S., Basu D., Fuller N., 1990, MNRAS, 244, 357
Robinson A., 1995, MNRAS, 272, 647
Stirpe G. M., 1990, A&AS, 85, 1049, S90
Stirpe G. M., 1991, A&A, 247, 3
Sulentic J. W., 1989, ApJ, 343, 54
van Groningen E., 1984, Ph. D. Thesis, Sterrewacht Leiden
Véron-Cetty M.-P., Véron P., 1984, A Catalogue of Quasars and Active Nuclei, ESO Sci. Rep. No. 1
Véron-Cetty M.-P., Véron P., 1989, A Catalogue of Quasars and Active Nuclei (4th Edition), ESO Sci. Rep. No. 7
Vrtilek J. H., Carleton N. P., Huchra H. P., 1981, BAAS, 13, 521
Wilson A., Heckman T., 1985, in Miller J. S., ed., Astrophysics of Active Galaxies and Quasi-Stellar Objects. University Science Books, Mill Valley, CA, p. 39
Zheng W., Binette L., Sulentic J. W., 1990, ApJ, 365, 115
Zwitter T., Calvani M., 1994, MNRAS, 270, L27

This paper has been produced using the Royal Astronomical Society/Blackwell Science LaTeX style file.